PNAS RESEARCH ARTICLE | EVOLUTION OPEN ACCESS

The circadian demethylation of a unique intronic deoxymethylCpG-rich island boosts the transcription of its cognate circadian clock output gene

Nisha Misra[a,1], Manohar Damara[a,1], Tao Ye[a], and Pierre Chambon[a,b,c,2]

Contributed by Pierre Chambon; received August 16, 2022; accepted December 22, 2022; reviewed by Denis Duboule and Filippo M. Rijli

We demonstrate that there is a tight functional relationship between two highly evolutionary conserved cell processes, i.e., the circadian clock (CC) and the circadian DNA demethylation–methylation of cognate deoxyCpG-rich islands. We have discovered that every circadian clock-controlled output gene (CCG), but not the core clock nor its immediate-output genes, contains a single cognate intronic deoxyCpG-rich island, the demethylation–methylation of which is controlled by the CC. During the transcriptional activation period, these intronic islands are demethylated and, upon dimerization of two YY1 protein binding sites located upstream to the transcriptional enhancer and downstream from the deoxyCpG-rich island, store activating components initially assembled on a cognate active enhancer (a RORE, a D-box or an E-box), in keeping with the generation of a transcriptionally active condensate that boosts the initiation of transcription of their cognate pre-mRNAs. We report how these single intronic deoxyCpG-rich islands are instrumental in such a circadian activation/repression transcriptional process.

circadian clock (CC) | circadian DNA demethylation-methylation | intronic deoxyCpG islands | YY1 protein | circadian transcription

Significance

How the conserved Circadian Clock (CC) and the circadian DNA demethylation of deoxyCpG islands exert a circadian transcriptional control of the CC output genes (CCG's) is unknown. We now reveal the presence of a single intronic deoxymethylCpG island in every CCG, but not in the CC nor their immediate output genes and demonstrate that these islands undergo demethylation coinciding with the circadian gene expression. Moreover, the circadian binding of the YY1 "bridging" protein is mandatory for an enhancer-CpG island crosstalk, leading to the generation of a transcriptionally active enhancer-CpG island condensate. In short, we reveal how the circadian DNA demethylation of intronic deoxyCpG islands cooperates with cognate CC enhancers to boost the transcription of the circadian genes and their expression.

The methylation of the cytosine residues within DNA deoxyCpG dinucleotides is an established epigenetic modification conserved from primordial organisms to modern eukaryotes (1–3). DNA methylation which is essential for mammalian development, as evidenced by the early lethality of mice lacking DNA methyltransferases (4, 5), has been implicated in genomic imprinting (6), X chromosome inactivation (7), and repression of both transposons (8) and germline-specific genes (9). Furthermore, DNA deoxyCpG methylation could be instrumental in the regulation of gene expression (10, 11) through chromatin remodeling (12, 13) and repression of transcription (14, 15). On the other hand, the circadian clock (CC) is an evolutionary-conserved mechanism which, through a series of transcriptional-translational feedback loops, regulates the expression of the circadian clock-controlled genes (16, 17, 18).

While both the DNA deoxyCpG methylation and the CC have evolved for more than 2 billion years and are known to be physiologically relevant, little is known concerning their functional relationship. Contrasting with evidence supporting the involvement of circadian oscillations in the binding of methylated histones (19, 20, 21), the role played by DNA deoxyCpG methylation–demethylation in the maintenance and modulation of the CC is still unclear. Indeed, it has been reported that modifications in the pattern of "DNA deoxyCpG methylation–demethylation" can be modulated in the mouse supra-chiasmatic nucleus through modification of the length of the CC period (22), and Clarkson-Townsend et al. (23) have shown that a "Maternal disruption of the circadian clock during night-shift work results into a change in the methylation pattern of the placental DNA."

In the present study, we demonstrate that there is a tight functional relationship between the CC and the alternate DNA deoxyCpG methylation–demethylation. We have identified in all circadian clock-controlled output genes (CCG's), a single cognate methylated intragenic intronic region (hereafter referred to as a "CpG island") which undergoes a circadian demethylation–methylation. Interestingly, this circadian island demethylation/methylation is concomitant with the diurnal alternate transcriptional activation/repression of their cognate circadian output genes.

Results and Discussion

A Single "Intronic deoxyCpG-Rich Island" Undergoing a Circadian Demethylation–Methylation Is Present within Each CC-Controlled Output Gene Containing a D-Box, a RORE, or an E-Box, but Not within the "Core Clock" Genes, Nor Their Immediate Output Genes. DNA purified from the mouse liver or ileum was fragmented by ultrasonication and the deoxyCpG- methylated DNA was immunoprecipitated with an antibody specific

Author contributions: N.M., M.D., and P.C. designed research; N.M., M.D., and T.Y. performed research; N.M., M.D., T.Y., and P.C. analyzed data; and N.M., M.D., and P.C. wrote the paper.

Reviewers: D.D., Ecole Polytechnique Federale de Lausanne; and F.M.R., Friedrich Miescher Institute for Biomedical Research.

The authors declare no competing interest.

[1]N.M. and M.D. contributed equally to this work.

[2]To whom correspondence may be addressed. Email: chambon@igbmc.fr.

This article contains supporting information online at https://www.pnas.org/lookup/suppl/doi:10.1073/pnas.2214062120/-/DCSupplemental.

Published February 15, 2023.

for 5-methyldeoxycytosine (5-mC). Analyses of the MethylDNA immunoprecipitate (MeDIP) through deep-parallel DNA sequencing (MeDIP-seq data; for example, see Fig. 1 *A*–*C* and *SI Appendix*, Fig. S1 *A* and *B*) revealed the presence of 200 to 1,500 bp-long differentially methylated deoxyCpG-rich genomic intronic regions (named hereafter "CpG islands": 859 in the liver, 446 in ileum), which were highly methylated either at ZT02 (8 AM, i.e., 2 h after the start of the circadian rest phase) or at ZT14

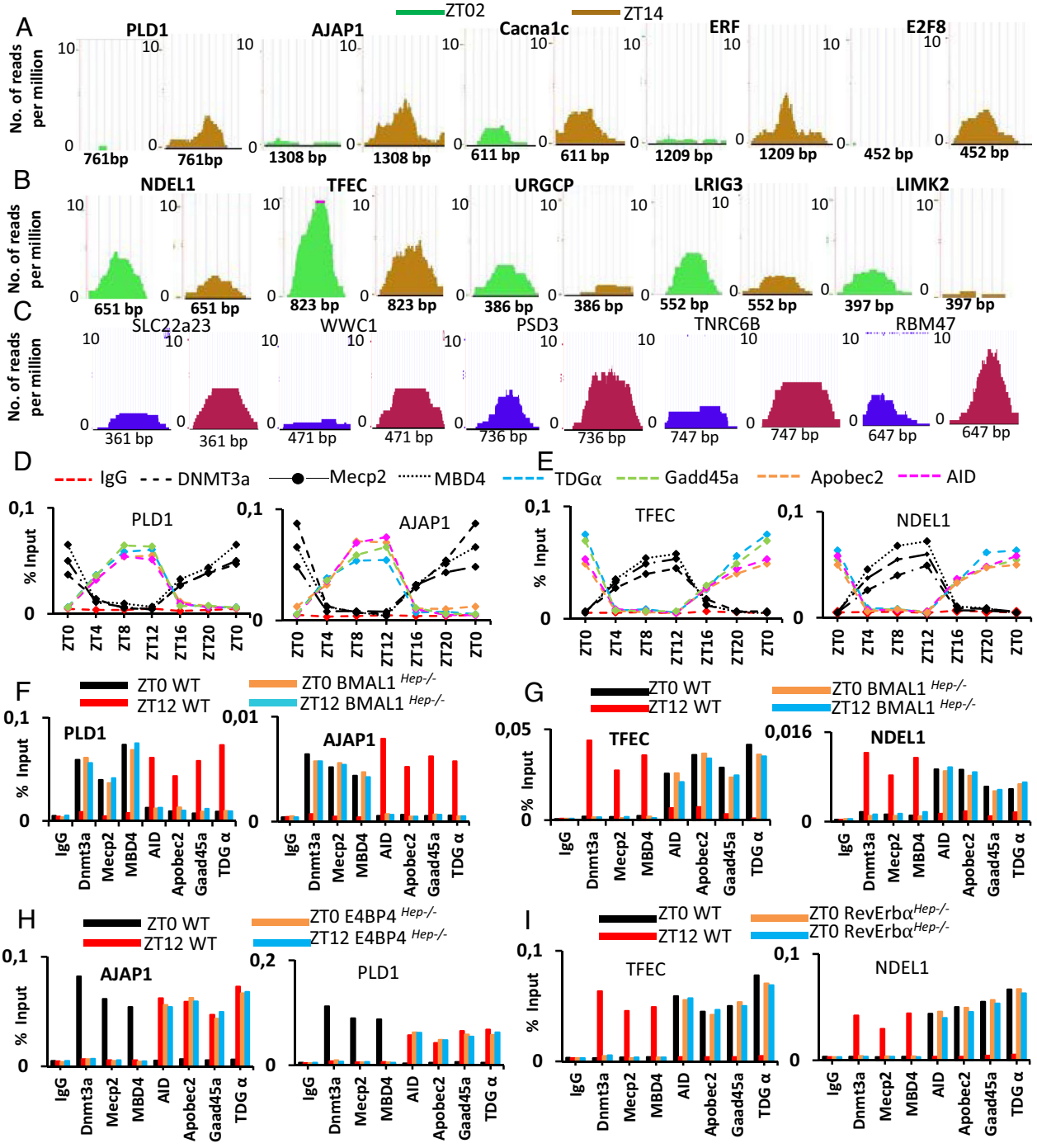

Fig. 1. The circadian alternate expression/repression of CC-controlled output genes is concomitant with the circadian alternate demethylation/methylation of their cognate intronic CpG islands (*A*) Genome browser view of liver CpG islands present in D-Box-containing output genes which are methylated at ZT14 and demethylated at ZT02. The methylation "signal" at ZT02 and ZT14 is represented as "reads per million," while the x-axis indicates the length (in base pairs) of the CpG islands. (*B*) as in (*A*), but for CpG islands of RORE-containing output genes which are methylated at ZT02 and demethylated at ZT14. (*C*) as in (*A*), but for CpG islands of E-box-containing output genes which are methylated at ZT14 and demethylated at ZT02. (*D*) qPCR chip assays with WT liver extracts, showing the circadian alternate binding of DNA methylating (DNMT3a, MeCP2, MBD4) and DNA demethylating enzymes (TDGα, GADD45a, Apobec2, and AID) to CpG islands of D-Box-containing genes, as indicated. (*E*) As in (*D*), but for RORE-containing genes, as indicated. (*F*) qPCR chip assays on liver extracts of BMAL1$^{hep-/-}$ mice, showing at ZT0 and ZT12 a constitutive binding of DNA methylating enzymes and a loss of binding of DNA demethylating enzymes on CpG islands of D-box-containing genes, as indicated. (*G*) qPCR chip assays on liver extracts of BMAL1$^{hep-/-}$mice, showing at ZT0 and ZT12 a loss of binding of DNA methylating enzymes and a constitutive binding of DNA demethylating enzymes on CpG islands of RORE-containing genes, as indicated. (*H*) qPCR chip assays on liver extracts of E4BP4$^{hep-/-}$mice, showing at ZT0 and ZT12 a constitutive binding of DNA demethylating enzymes on CpG islands of D-box-containing genes, as indicated. (*I*) as in (*G*), but with liver extracts of RevErbα$^{hep-/-}$mice on CpG islands of RORE-containing genes, as indicated.

(8 PM, i.e., 2 h after the start of the active phase). Such a single intronic phosphorylated cytosine guanidine (CpG)-rich island was present within 281 RORE- and 247 D-Box-containing genes in the liver (*SI Appendix*, Tables S1 and S2) and within 202 RORE- and 244 D-box-containing genes in ileum (*SI Appendix*, Tables S3 and S4), of which 21% exhibited the same circadian methylation profile as in the liver (see *SI Appendix*, Table S5; note that islands shorter than ~200bp would escape detection; see below). This profile was characterized by a zenith at ~ZT14 and a nadir at ~ZT02 for D-Box genes (Fig. 1*A* and *SI Appendix*, Fig. S1*A*), while an inverse profile (zenith at ~ZT02, nadir at ~ZT14) was observed for RORE genes (Fig. 1*B* and *SI Appendix*, Fig. S1*B*). Importantly, each of these CpG islands is located in a cognate intronic region (*SI Appendix*, Tables S1–S4 and S6 *B–F*). Strikingly, none of the "core clock" genes (BMAL1, CLOCK, RORγ, RevErbα, PER1/2, and CRY1/2), nor the D site of albumin promoter (albumin D-box) binding protein (DBP) and E4BP4 "immediate" output genes (Fig. 4*C*), were found among liver and ileum MeDIP-seq data, at either ZT02 or ZT14. Accordingly, ENSEMBLE gene sequence analyses (http://feb2014.archive.ensembl.org) did not reveal in mice, nor in humans, the presence of intragenic CpG islands within the core clock and clock-controlled immediate output genes (*SI Appendix*, Tables S6*A* and S10).

That CC output genes containing either a RORE or a D-box consensus site harbor a CpG island undergoing a circadian alternate DNA demethylation/methylation (Fig. 1 *A* and *B*) prompted us to investigate whether similar CpG islands could be present in E-box-containing output genes controlled by the "core clock" BMAL1 gene. Screening both a public mouse liver database for BMAL1 chip-seq and RNA-seq data (24) (Accession no: GSE110604), and our own liver MeDIP-seq data (Accession no: GSE182147), revealed the presence of intragenic intronic CpG islands in 331 Bmal1-activated "E-box output genes" (*SI Appendix*, Table S7) exhibiting a circadian DNA demethylation/methylation profile (Fig. 1*C*), in keeping with the "chip-seq" circadian profile of BMAL1 binding to its E-box cognate site.

The RNA transcript levels of 20 D-Box and 20 RORE genes (randomly selected within our liver MeDIP-seq data) were determined by qPCR every 4 h during 24 h. The zenith of these RNA transcripts occurred between ZT8–ZT12 for D-Box genes (*SI Appendix*, Fig. S1*C* and Table S8*A*), i.e., at a time when little DNA methylation of the CpG islands could be detected, whereas their nadir was correlated with maximum DNA methylation at ZT14. An inverse correlation (i.e., RNA transcript zenith at ZT0–ZT20, maximum DNA methylation at ZT02) was observed for RORE genes (*SI Appendix*, Fig. S1*D* and Table S8*B*). Such correlations between high/low levels of RNA transcripts and demethylation/methylation of CpG islands were further supported by chip analyses which indicated a 12-h circadian alternance between the bindings of both DBP and E4BP4 to D-box DNA binding sequence (DBS) (*SI Appendix*, Fig. S1*D*) and of both RORγ and RevErbα to RORE DBS (*SI Appendix*, Fig. S1*D*). As expected, RORα did not bind to RORE sites in the liver (25, 26) (*SI Appendix*, Fig. S1*D*).

Knowing that, in the liver, the CC output genes which contain a RORE are activated by RORγ and repressed by RevErbα (Fig. 4*C*), we compared our list of RORE-activated genes harboring a CpG island with the list of 238 RORE-containing genes which were found to be repressed by RevErbα in the liver (27). This comparison indicated that 198 of these RevErbα-repressed genes were present in our list of RORE-activated genes (*SI Appendix*, Table S1). "ENSEMBLE" gene sequence analyses (http://feb2014.archive.ensembl.org) of the 40 RevErbα-repressed genes not found in our RORE list revealed either i) the lack of an intronic CpG-rich region within these genes or ii) the presence of a short intronic CpG-rich region which was below the limit of sensitivity of our Medip-seq analysis which did not allow the detection of CpG-rich regions that are less than 200 bp long (*SI Appendix*, Table S9).

It is known that "circadian output genes" involved in a given physiological function are coexpressed during a defined diurnal period (16). For example, the liver synthesizes and stores nutrients during the circadian active phase and tap into them during the rest phase. Our MeDIP-seq data showed that the CpG islands present in RORE-containing genes involved in glucose catabolism and lipid anabolism were demethylated during the circadian active phase, while they were methylated during the rest phase (*SI Appendix*, Table S1). In contrast, the CpG islands present in D-box-containing genes involved in lipid catabolism were methylated during the active phase, while they were demethylated during the rest phase (*SI Appendix*, Table S2), indicating that the circadian alternate methylation/demethylation of the CpG islands could be physiologically relevant and instrumental in the molecular mechanisms underlying the CC.

Taken altogether, the above data demonstrate that all CC-controlled output genes, but not the core clock genes nor their immediate output genes, contain a single intronic CpG-rich island that undergoes a circadian demethylation–methylation which is concomitant with i) the circadian alternate bindings of a transactivator and a transrepressor to a cognate enhancer and ii) the circadian alternate activation/repression of transcription of the CC output genes.

The Alternate Demethylation–Methylation of the Intronic CpG-Rich Islands Is Controlled by the Circadian Core Clock. Chip assays showed that the DNMT3a, MeCP2, and MBD4 enzymes, known to be instrumental in CpG methylation (5, 28), are maximally bound at ZT0 (6 AM) to the CpG islands of D-box output genes (Fig. 1*D* and *SI Appendix*, Fig. S1*D*; i.e., at a time when the messenger ribonucleic acid (mRNAs) expression of these rest phase genes is at its nadir; *SI Appendix*, Fig. S1*C*). On the other hand, enzymes involved in active demethylation (29, 30) (i.e., TDGα, GADD45α, AID, and Apobec2) are optimally bound to the same CpG islands at ZT12 (6 PM) (Fig. 1*D* and *SI Appendix*, Fig. S1*D*), i.e., at a time at which the RNA transcript levels of D-box genes is at its zenith (*SI Appendix*, Fig. S1*C* and Fig. 4*B*). Reciprocally, the DNMT3a, MeCP2, and MBD4 CpG methylating enzymes are maximally bound to the CpG islands of RORE-containing output genes at ZT12 (6 PM) (Fig. 1*E* and *SI Appendix*, Fig. S1*E*), i.e., when the RNA transcript levels of these active phase genes is at its nadir (*SI Appendix*, Fig. S1*D*), whereas enzymes involved in active demethylation (TDGα, GADD45α, AID, and Apobec2) are optimally bound to the same CpG islands at ZT0 (6 AM) (Fig. 1*E* and *SI Appendix*, Fig. S1*E*), i.e., when the mRNA expression of RORE genes is at its zenith (*SI Appendix*, Fig. S1*D* and Fig. 4*A*). Taken altogether, these data indicate that the alternate demethylation/methylation of the CpG islands is under the control of the circadian core clock.

To unequivocally support the above conclusion, we in vivo selectively mutated in mouse hepatocytes either one of the core clock genes BMAL1 and RevErbα or the E4BP4 immediate output gene. In BMAL1$^{hep-/-}$ mutant mice, due to the constitutive activity of E4BP4 (*SI Appendix*, Fig. S1*G*; see Fig. 4*C*) which represses the expression of the D-Box genes (*SI Appendix*, Fig. S1*H*), the CpG methylating enzymes were constitutively bound to the CpG islands of the repressed D-box genes (Fig. 1*F*). In contrast, upon mutation of the E4BP4 repressor (E4BP4$^{hep-/-}$mutant mice), the permanent binding of DBP to its cognate D-box DBS (*SI Appendix*, Fig. S1*I* and Fig. 4*C*) resulted in a constitutive binding of the demethylating

enzymes to CpG islands (Fig. 1*H*), thereby leading to the constitutive expression of D-box genes (*SI Appendix*, Fig. S1*J*). Furthermore, in either BMAL1$^{hep-/-}$ (*SI Appendix*, Fig. S1*K*) or RevErbα$^{hep-/-}$ (*SI Appendix*, Fig. S1*L*) mutant mice, the permanent binding of RORγ to its cognate RORE DBS led to the constitutive binding of demethylating enzymes to CpG islands (Fig. 1 *G* and *I*), which was correlated with a constitutive expression of the RORE genes (*SI Appendix*, Fig. S1 *M* and *N*; see Fig. 4*C*).

DNA analyses through bisulphite sequencing unequivocally confirmed that the circadian alternate methylation/demethylation of cytosine residues within CpG islands of D-box genes (*SI Appendix*, Fig. S3*A*) occurred during the periods of optimal binding of methylating (at ZT14) and demethylating (at ZT02) enzymes (Fig. 1*D*). Similar analyses within CpG islands of RORE genes (*SI Appendix*, Fig. S3*B*) revealed ZT02 and ZT14 zeniths for the methylation and demethylation of the CpG residues, in phase with the alternate binding of methylating and demethylating enzymes (Fig. 1*E*). These bisulphite analyses also showed that none of the few CpGs which are located in the vicinity of the RORE and D-Box enhancer regions of the core clock genes (RevErbα, BMAL1, and PER1; *SI Appendix*, Fig. S3*C*) and of their CC output genes (*SI Appendix*, Fig. S3 *D* and *E*) were significantly methylated at ZT0 and ZT12.

We conclude from the above data that even though the enzyme activities involved in the circadian DNA demethylation (TDGα, GADD45α, AID, and Apobec2) and methylation (DNMT3a, MeCP2, and MBD4) of the CpG islands are constitutive, their bindings to the CpG islands present within D-box and RORE genes are controlled by the circadian core clock repressors RevErbα and E4BP4, thereby leading to the circadian alternate methylation–demethylation of these islands.

Components Known to Be Associated with "Active Chromatin" Are Concomitantly Associated with Both "Active Enhancers" and Demethylated Intronic CpG Islands. We examined whether, 4 h before the start of pre-mRNA transcription, the three histone demethylases/acetylases (JARID1a, KDM6a, and JHDM3a) and the acetylated histones which are known to be associated with enhancers could also be detected on the CpG islands of D-box and RORE output genes (Fig. 2 *A* and *B* and *SI Appendix*, Fig. S5*A*). We found such "CpG island circadian associations" of i) JARID1a (an H3K4Me3 histone-specific demethylase), known to inhibit the binding of HDACs (31) and of ii) KDM6a and JHDM3a which selectively demethylate/acetylate the H3K27Me3 and H3K9Me3 histones (32, 33) to H3K27Ac and H3K9Ac, respectively, the zeniths of which were between ZT8 and ZT12 for D-box genes (Fig. 2*A*) and ZT20 and ZT0 for RORE genes (Fig. 2*B*). In keeping with these data, chip assays on CpG islands revealed the circadian histone modifications of H3K9Ac, as well as of histones modifications known to be hallmarks of "active enhancers" (H3K27Ac and H3K4Me1), with zeniths between ZT8 and ZT12 for D-box genes (Fig. 2*C*) and ZT20 and ZT0 for RORE genes (Fig. 2*D*). Similarly, H3K9Ac and active enhancer-

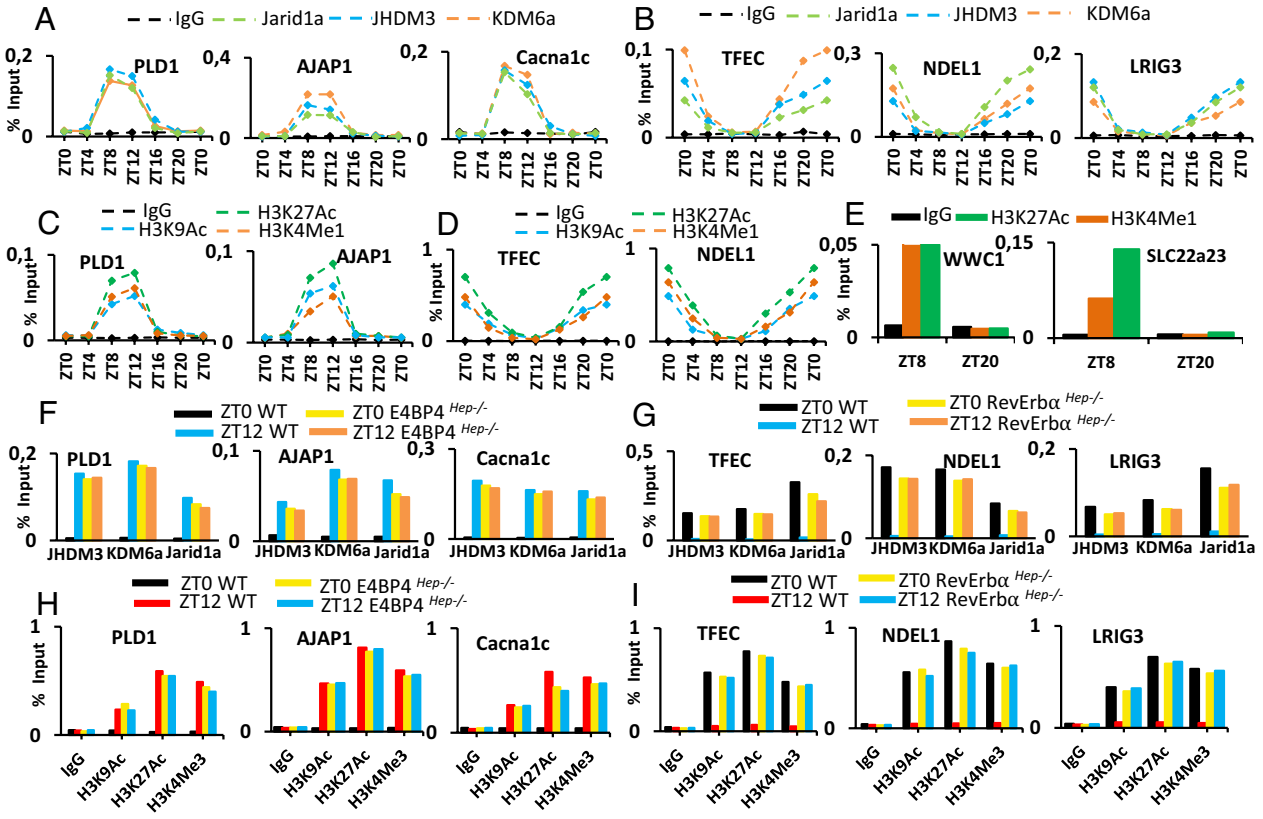

Fig. 2. The main components of active chromatin are concomitantly associated with enhancers and demethylated CpG islands. (*A* and *B*) qPCR chip assays with WT liver extracts showing the circadian recruitment of JARID1a, JHDM3, and KDM6a demethylases on CpG islands of D-Box (Fig. 2*A*) and RORE (Fig. 2*B*)-containing genes, as indicated. (*C* and *D*) qPCR chip assays with WT liver extracts showing the circadian binding of histone H3K9Ac and enhancer-specific histones (H3K27Ac and H3K4Me1) on CpG islands of D-box (Fig. 2*C*) and RORE-containing (Fig. 2*D*) genes, as indicated. (*E*) qPCR chip assays with WT liver extracts showing the circadian binding of H3K27Ac and H3K4Me1 to CpG islands of two E-box-containing genes, as indicated. (*F*) qPCR chip assays showing, in E4BP4$^{hep-/-}$ mice, the "constitutive" binding of JARID1a, JHDM3, and KDM6a on CpG islands of D-Box-containing genes, as indicated. (*G*) qPCR chip assays showing, in RevErbα$^{hep-/-}$ mice, the "constitutive" binding of JARID1a, JHDM3, and KDM6a on CpG islands of RORE-containing genes, as indicated. (*H* and *I*) As under (*C* and *D*), but for CpG islands of D-box-containing genes in E4BP4$^{hep-/-}$ mice (Fig. 2*H*) and of RORE-containing genes in RevErbα$^{hep-/-}$mice (Fig. 2*I*), as indicated.

specific histones were found on D-box and RORE enhancer regions of CC output genes (*SI Appendix*, Fig. S2 *K* and *L*). In addition, the bindings of the above histone demethylases and active enhancer-specific histone modifications to CpG islands of D-box (Fig. 2 *F* and *H*) and RORE (Fig. 2 *G* and *I*) genes were constitutive in E4BP4$^{hep-/-}$ and RevErbα$^{hep-/-}$ mutant mice. Of note, the histone variants H3.3 (34–36) and H2A.Z (37, 38), known to be enriched on enhancers, were similarly detected on the CpG islands of D-box and RORE genes (*SI Appendix*, Fig. S2 *M* and *N*), while constitutively bound in E4BP4$^{hep-/-}$ and RevErbα$^{hep-/-}$ mutant mice (*SI Appendix*, Fig. S2 *O* and *P*).

Components Known to Be Associated with Transcriptional Enhancer–Mediator Complexes Are Concomitantly Present on Their Cognate Demethylated Intronic CpG Islands. Surprisingly, even though no RORE nor D-Box binding sites could be found within the CpG islands, chip assays revealed the circadian presence of RORγ and DBP transactivators not only on their cognate enhancers (Fig. 3 *A* and *B*) but also on their respective CpG islands, with zeniths between ZT20 and ZT0 for RORE genes (Figs. 3*A* and 4*A*) and ZT8 and ZT12 for D-box genes (Figs. 3*B* and 4*B*). Moreover, we found that CBP, P300, and RNA polymerase II (RNAPII), all of which known to be associated with transcriptional enhancers and instrumental in the expression of genes involved in the circadian cycle (21), were similarly present within the intronic demethylated CpG islands, with zeniths between ZT8 and ZT12 for D-box (Fig. 3*D*) and ZT20 and ZT0 for RORE (*SI Appendix*, Fig. S2*A*) genes. All of these CpG island associations were concomitant with those observed on D-box and RORE enhancers and preceded the associations of CBP, P300 (*SI Appendix*, Fig. S2 *C* and *D*), and RNAPII (*SI Appendix*, Fig. S2 *E* and *F*) to the proximal promoter region, while "constitutive" upon mutation of the transrepressors (E4BP4$^{hep-/-}$ mice for D-box genes and RevErbα$^{hep-/-}$ mice for RORE genes; see Fig. 3*E* and *SI Appendix*, Fig. S2*B*).

Mediator complexes are multisubunit complexes of MED proteins, acting as functional bridges facilitating the interaction between enhancer-bound transcription factors and preinitiation complexes (PIC) located within the proximal promoter region of target genes (39, 40). Whether MED proteins, which are initially associated with enhancers and then with proximal promoter regions, could also be present within the CpG islands of D-box and RORE-containing genes, was investigated through chip assays with two MED antibodies. The binding zeniths of MED1 (Fig. 3 *G* and *H*) and MED12 (Fig. 3 *I* and *J*) on enhancers and demethylated CpG islands were at ZT8–ZT12 for D-box genes (Fig. 3 *G* and *I*) and at ZT20–ZT0 for RORE genes (Fig. 3 *H* and *J*), thus preceding by 4 h their recruitment on the proximal promoter region (Fig. 3 *G*–*J*). Of note, these MED1 and MED12 mediator bindings to the CpG islands coincided with the simultaneous

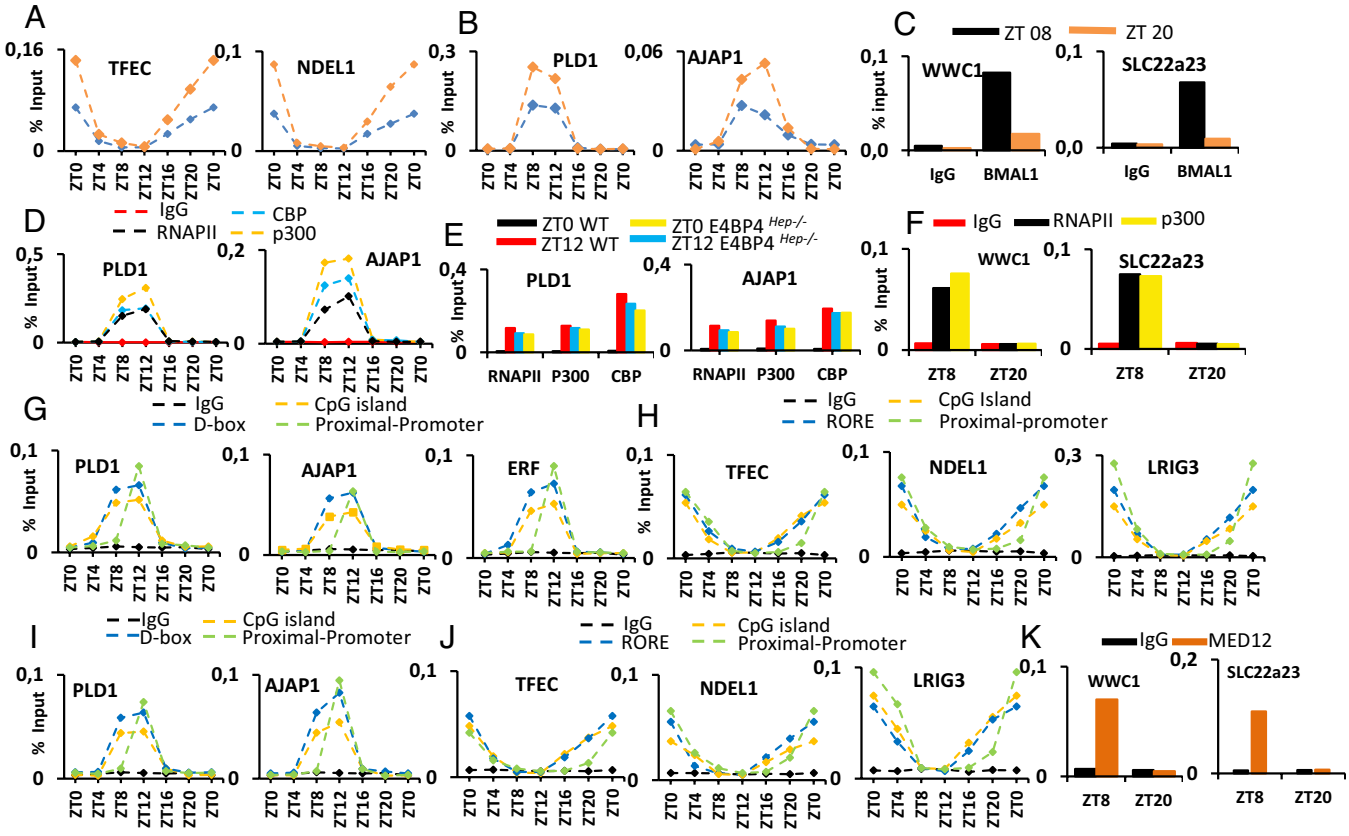

Fig. 3. The main components of transcriptional enhancer/mediator complexes are concomitantly associated with enhancers and demethylated CpG islands (*A*) qPCR chip assays with WT liver extracts, showing the concomitant circadian presence of RORγ on both the CpG island (blue) and RORE enhancer (orange) of CC output genes, as indicated. (*B*) As under (*A*), but for the circadian binding of DBP to the CpG island (blue) and the D-box enhancer (orange) of CC output genes, as indicated. (*C*) As under (*A*), but for the circadian association of BMAL1 at ZT8 and ZT20 to the CpG islands of two E-box-containing genes, as indicated. (*D*) qPCR chip assays with WT liver extracts showing the circadian recruitment (ZT8) of RNAPII, CBP, and p300 on CpG islands of D-box-containing genes, as indicated. (*E*) As under (*D*), but for CpG islands of D-box-containing genes in E4BP4$^{hep-/-}$ mice. (*F*) qPCR chip assays with WT liver extracts showing the circadian binding of RNAPII and P300 on CpG islands of E-box-containing genes, as indicated. (*G* and *I*) qPCR chip assays showing, in WT liver extracts, the circadian recruitments of MED1 (Fig. 2*G*) and MED12 (Fig. 2*I*) on CpG islands, D-Box enhancer, and proximal promoter region of genes, as indicated. (*H* and *J*) As under (Fig. 2 *G* and *I*), but for RORE-containing genes, as indicated. (*K*) qPCR chip assays showing, in WT liver extracts, the circadian binding of MED12 to the CpG islands of two E-box-containing genes, as indicated.

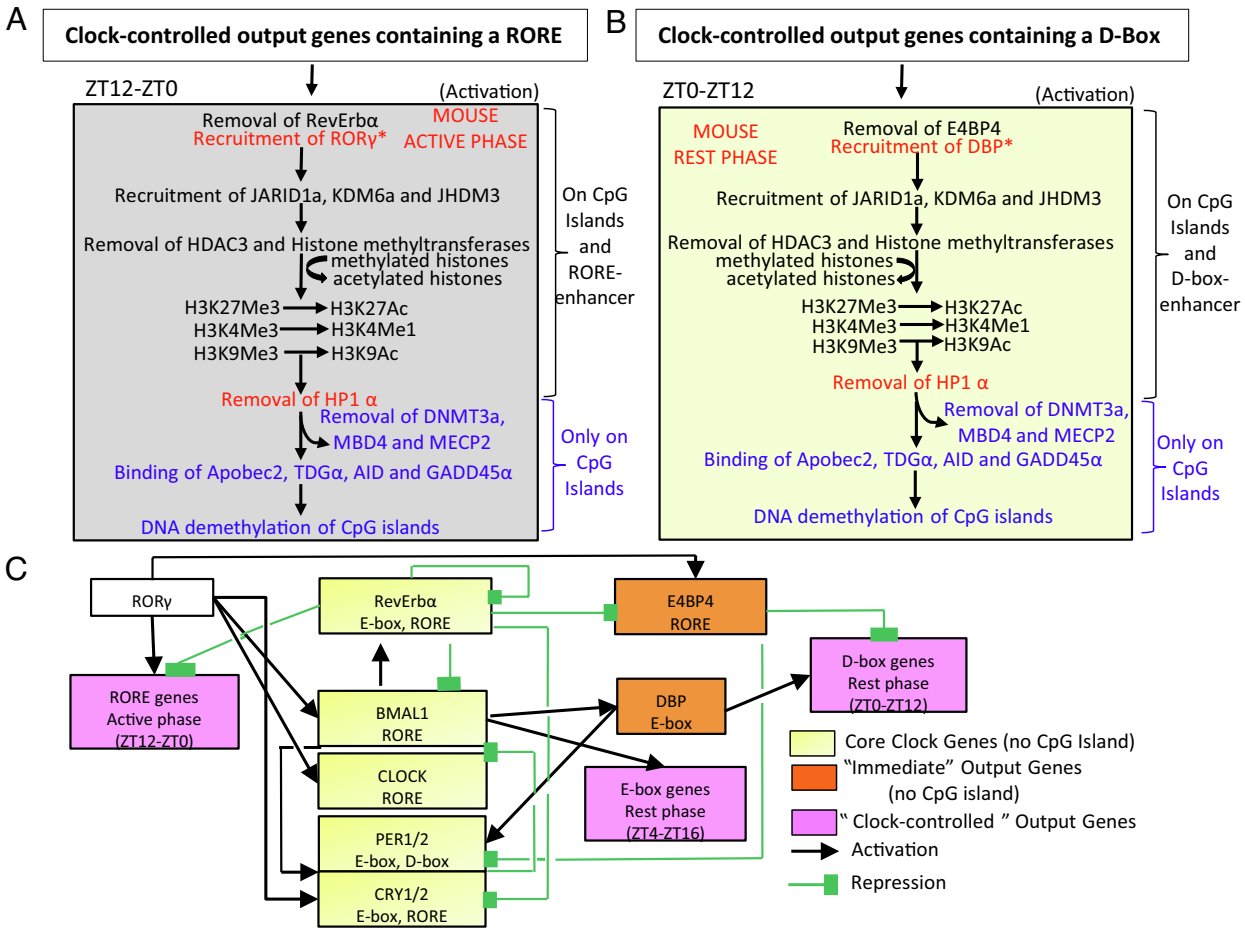

Fig. 4. (*A*) Schematic representation showing, in the liver, the mechanism through which the DNA demethylation of CpG islands control the circadian expression of RORE-containing output genes. The asterisk (*) indicates a nonspecific binding on CpG islands. (*B*) Schematic representation showing, in the liver, the mechanism through which the DNA demethylation of CpG islands control the circadian expression of D-box-containing output genes. The asterisk (* as under *A*) indicates a nonspecific binding on CpG islands. (*C*) Schematic representation of the CC. The core clock genes are shown on a yellow background, the "immediate" output genes (DBP and E4BP4) are on an orange background, and the clock-controlled output genes (D-box, RORE and BMAL1-dependent E-box genes) are on a pink background. Black arrows indicate "activation" and green bars "repression" of transcription, respectively.

presence of P300, CBP, and RNA polymerase (RNAPII) on both enhancer and CpG islands (Fig. 3*D* and *SI Appendix*, Fig. S2 *A* and *C–F*). Similarly, the BRD4 protein, known to be associated with MED1 (41, 42), was found to be initially recruited on D-box (*SI Appendix*, Fig. S2*I*) and RORE (*SI Appendix*, Fig. S2*J*) enhancers, as well as on their cognate CpG islands (*SI Appendix*, Fig. S2 *I* and *J*), with zeniths between ZT8 and ZT12 for D-box genes and ZT20 and ZT0 for RORE genes, i.e., before its final recruitment on the proximal promoter region (*SI Appendix*, Fig. S2 *I* and *J*).

Taking the above data altogether (*SI Appendix*, Fig. S5), we conclude that the binding of the CC transactivators RORγ and DBP to their cognate enhancers is accompanied by their presence on the CpG islands, even though these islands are devoid of cognate binding sites. Furthermore, our "chip data" indicate that upon demethylation, the CpG islands which are present within D-box- and RORE-containing genes exhibit a hydrophilic surface on which components known to be present on enhancer–mediator regions do bind (41, 43–47) (i.e., transactivator, active enhancer-specific histones, RNAPII, CBP, P300, MED proteins, and BRD4).

Altogether our "chip data" indicate that all components known to be required for initiating transcription of the CC output genes are present not only on D-box and RORE enhancers but also on their cognate intronic CpG islands, at a time preceding the initiation of transcription from the proximal promoter region.

The Circadian Bindings of the YY1 "Bridging" Protein to Two Cognate Single Sites, Respectively, Located Upstream to the Enhancer and Downstream from the CpG Island of D-Box and RORE CC Output Genes, Precede Its Additional Binding to a Single Site Located within the Proximal Promoter Region. The YY1 (Yin Yang 1) protein is a "bridging" protein which, through DNA looping, is known to be required to generate physical interactions between enhancer/mediator complexes and proximal promoter regions (48). As on both the enhancer (*SI Appendix*, Fig. S2) and the demethylated CpG island (Figs. 2 and 3), the presence of enhancer/mediator components (e.g., CBP, P300, RNAPII, BRD4, and MED proteins) precedes their detection on the proximal promoter region, we investigated whether the "machinery" required for "active transcription" could be initially associated with both the enhancer and the CpG island, to be subsequently transferred on the proximal promoter region through "YY1-guided" looping.

Bioinformatic searches on circadian D-box and RORE genes which contain a CpG island and are expressed in either the liver (Fig. 5 *A* and *B*), ileum (Fig. 5 *C* and *D*), or in both tissues (Fig. 5 *E* and *F*) identified single consensus YY1 binding sites (48) (black filled circles and green bars) located both upstream to D-box or RORE enhancers and downstream from the CpG islands, as well as multiple YY1 sites located near the transcription start site (TSS; Fig. 5 *A–F*). For each of these D-box and RORE genes, a single enhancer binding site was located 1 to 13 kbs upstream from the

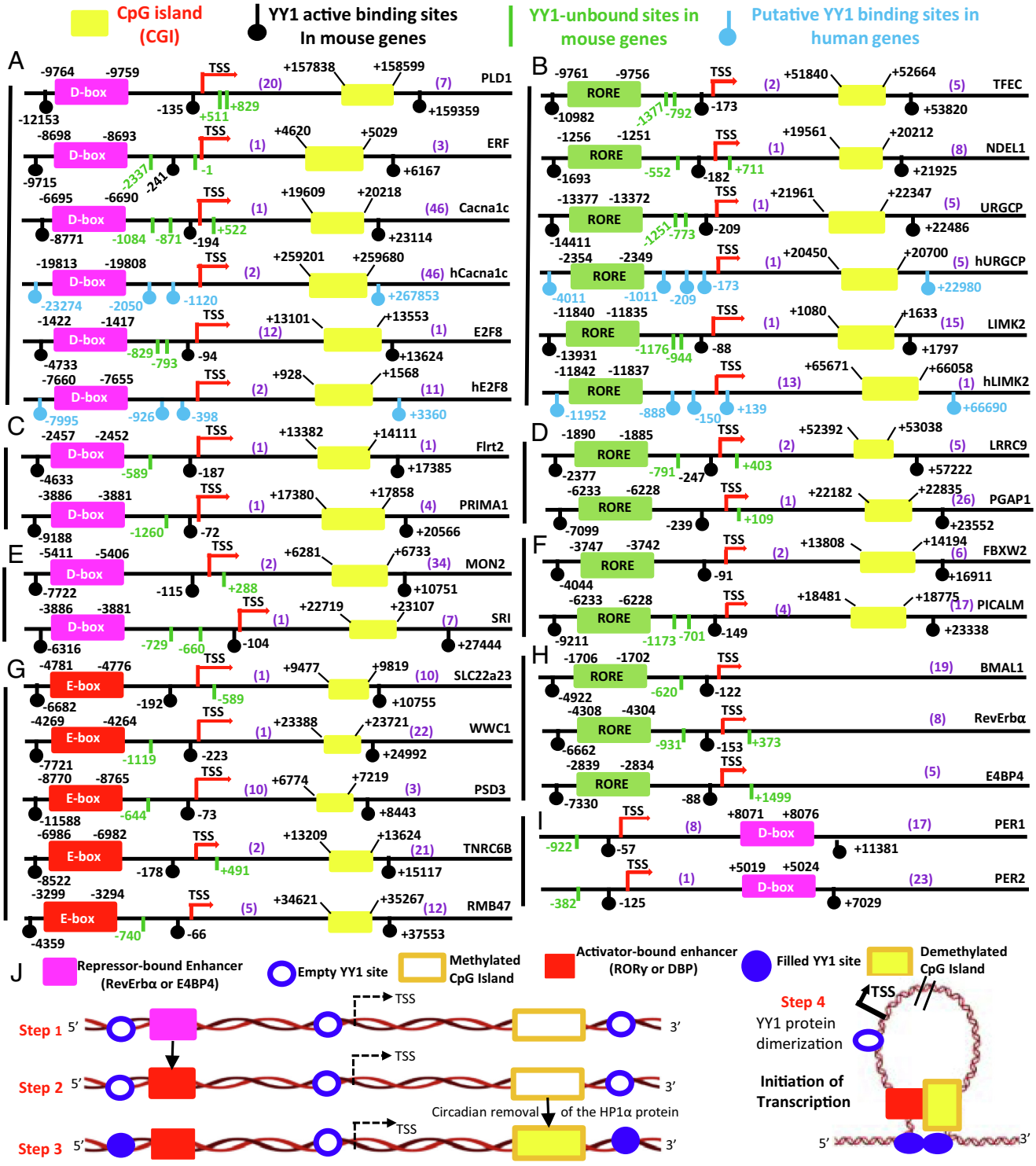

Fig. 5. Schematic representation of core clock genes and clock-controlled output genes expressed in the liver and ileum, showing the position of YY1 sites located near the CpG island, the enhancer, and the proximal promoter. (*A* and *B*) Schematic position of YY1 binding sites (see below) located near D-box (pink) and RORE (green) enhancers, CpG islands (yellow), and transcription startsite (TSS; red) for D-box (Fig. 5*A*) and RORE (Fig. 5*B*) genes expressed in the mouse liver and for D-box genes (hE2F8 and hCacna1c) and RORE genes (hLIMK2 and hURGCP) in human. The number of exons (in parenthesis) on both sides of the islands are indicated in purple. (*C* and *D*) As under (*A* and *B*), but for genes expressed in both liver and ileum. (*E* and *F*) As under (*A* and *B*), but for genes selectively expressed in ileum. (*G*) Schematic position of YY1 binding sites located close to E-box, CpG islands, and proximal promoter regions of BMAL1-dependent genes expressed in the liver. The number of exons (in parenthesis) are highlighted in purple. (*H* and *I*) Schematic position in the mouse of YY1 binding sites which are located close to RORE (Fig. 6*H*) and D-box (Fig. 6*I*) enhancers, and within the promoter proximal regions of core clock genes (BMAL1, RevErbα, PER1 and PER2) and of immediate output gene E4BP4. The number of exons (in parenthesis) are highlighted in purple. (*J*) Schematic representation of crosstalks between the enhancer-mediator region, the CpG island, and the proximal promoter region through YY1-guided loop formation during the circadian period of gene activation. Step 1: The gene is shown in a "linear repressed form" with empty YY1 binding sites, a repressor-occupied enhancer region and the methylated CpG-rich island; Step 2: Represents the binding of a transactivator to the enhancer region; Step 3: Represents the circadian removal of the HP1α protein which leads to the binding of the YY1 protein 5′ to the enhancer and 3′ to the CpG island and to the demethylation of the CpG island, before the start of transcription; and Step 4: Represents the dimerization of the YY1 proteins bound to its cognate sites located, respectively, upstream to the enhancer and downstream from the CpG island, and the "fusion of contents" associated with the enhancer–mediator region with those stored within the CpG island, before the start of transcription from the TSS.

TSS, while a single intronic CpG island was present 1 to 160 kbs downstream from the TSS (Fig. 5 *A*–*F*). Single consensus YY1 sites were found (a) 400 bp to 5 kbs upstream to the enhancer region, (b) 130 bp to 3 kbs downstream from the CpG island, while (c) multiple cognate YY1 binding sites were present within 1.5 kb upstream and 1.5 kb downstream from the TSS (Fig. 5 *A*–*F*).

Chip analyses (Fig. 6 *A* and *B*) revealed the circadian recruitment of the YY1 protein to two single YY1 binding sites, respectively, located upstream to the enhancer and downstream from the CpG

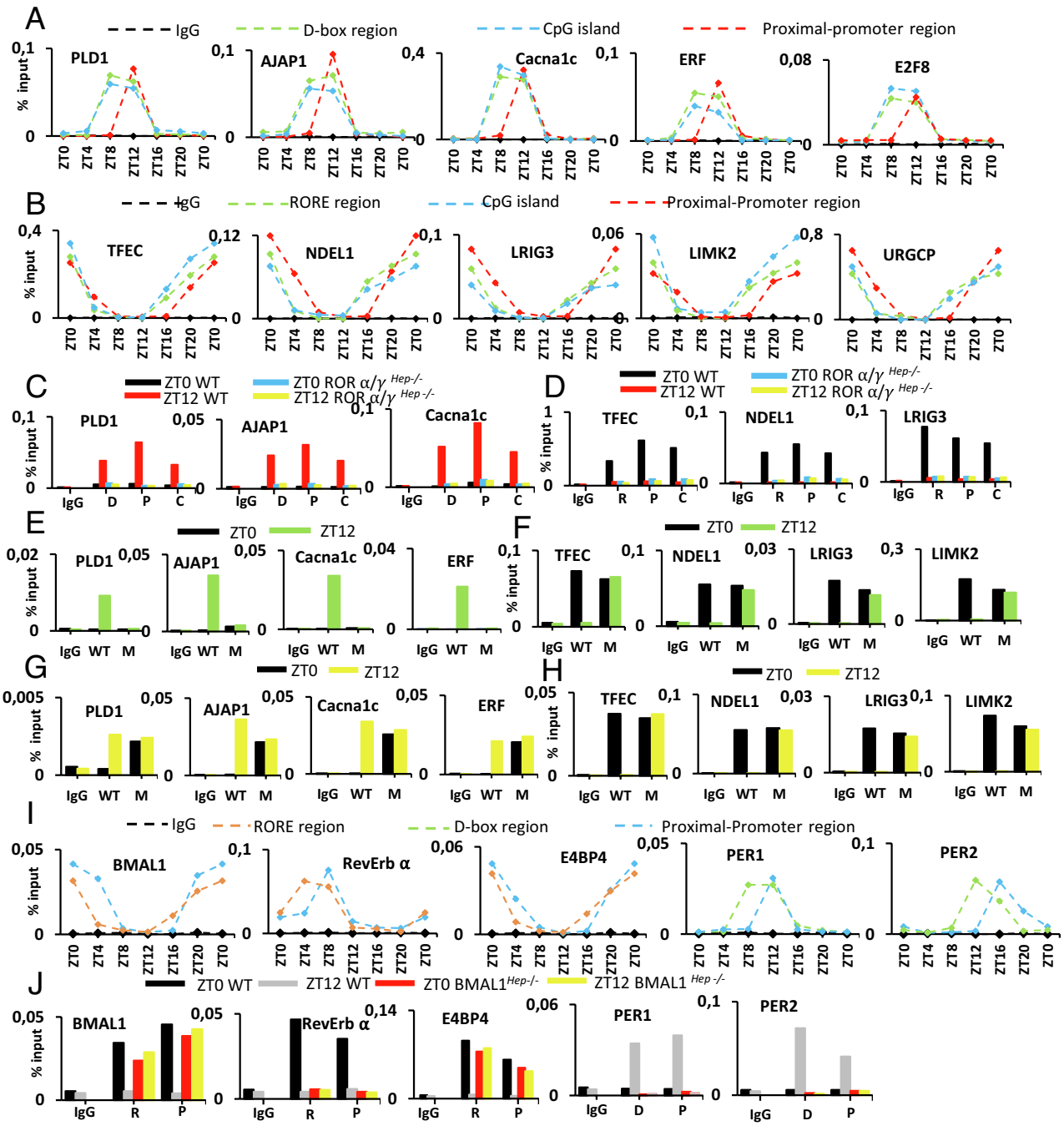

Fig. 6. The circadian binding of the YY1 protein to two unique YY1 cognate binding sites (located upstream to the enhancer region and downstream from the CpG islands) precedes its binding to an "active" site located within the proximal promoter region. (*A*) qPCR chip assays with WT liver extracts, indicating the circadian recruitment of the YY1 protein on YY1 consensus sites located near the CpG islands, the D-box enhancer, and within the proximal promoter regions of D-box-containing genes (Fig. 5*A*). (*B*) same as under (*A*), but for RORE-containing genes (Fig. 5*B*). (*C*) qPCR chip assays on liver extracts of RORα/γ$^{hep-/-}$ mice, showing the loss of recruitment of the YY1 protein on its cognate sites located close to the CpG islands (C), the D-box enhancers (D), and to the promoter regions (P) of D-box-containing genes. (*D*) qPCR chip assays on liver extracts of RORα/γ$^{hep-/-}$ mice, showing the loss of recruitment of the YY1 protein on its cognate sites located close to the CpG islands (C), the RORE enhancers (R), and to the promoter regions (P) of RORE-containing genes. (*E* and *F*) qPCR chip assays on liver extracts of BMAL1$^{hep-/-}$mice, showing the loss of circadian recruitment of the YY1 protein on its cognate site located near the CpG island of D-box (Fig. 6*E*) and RORE (Fig. 6*F*)-containing genes. WT and mutants are represented by WT and M, respectively. (*G* and *H*) qPCR chip assays showing, at both ZT0 and ZT12, the constitutive recruitment of the YY1 protein on its cognate sites located near the CpG islands of D-box-containing genes in E4BP4$^{hep-/-}$ mice (Fig. 6*G*) and RORE-containing genes in RevErbα$^{hep-/-}$ mice (Fig. 6*H*). WT and M, as under (*E* and *F*) (*I*) qPCR chip assays with WT liver extracts showing the circadian recruitment of the YY1 protein on YY1 consensus sites located upstream of RORE and D-box enhancers and on a single active site located within the proximal promoter region of core clock and immediate CC output genes (Fig. 5 *I* and *H*). (*J*) qPCR chip assays on liver extracts of BMAL1$^{hep-/-}$ mice, showing the role of BMAL1 in the binding of YY1 to RORE (R) and D-box (D) enhancers of core clock and immediate output genes.

island while, in the proximal promoter region, a single YY1 site was found to be functional (i.e., bound the YY1 protein) among several unbound sites (Figs. 5 *A* and *B* and 6 *A* and *B*). Note that the YY1 bindings located upstream to the enhancer and downstream from the CpG islands exhibited a ZT8–ZT12 zenith for D-box genes and a ZT20–ZT0 zenith for RORE genes (Fig. 6 *A* and *B*), thus preceding a further binding to the "functional" site located within the proximal promoter region (Fig. 6 *A* and *B* and *SI Appendix*, Fig. S6*A*). Furthermore, the circadian recruitments of the YY1 protein to these cognate sites were concomitant with the circadian "active phase" for genes expressed between ZT12 and ZT0 (the RORE genes) and within the "rest phase", for genes expressed between ZT0 and ZT12 (the D-box genes). Selective in vivo mutations in hepatocytes demonstrated that these YY1 recruitments were under the control of the CC: they were indeed lost in RORα/γ$^{hep-/-}$mice (Fig. 6 *C* and *D*) while, in BMAL1$^{hep-/-}$ mice (that lack both the DBP activator and the RevErbα repressor; see Fig. 4*C*), they were lost in D-box genes (Fig. 6*E* and *SI Appendix*, Fig. S6*B*) and constitutive in RORE genes (Fig. 6*F* and *SI Appendix*, Fig. S6*C*). As expected, in both E4BP4$^{hep-/-}$ and RevErbα$^{hep-/-}$ mutants (i.e., in the absence of a repressor), these YY1 recruitments were constitutive for both D-box (Fig. 6*G* and *SI Appendix*, Fig. S6*D*) and RORE (Fig. 6*H* and *SI Appendix*, Fig. S6*E*) genes.

Searches for clock-controlled output genes expressed in ileum (*SI Appendix*, Fig. S1 *A* and *B* and Fig. 5 *C* and *D*) or in both liver and ileum (Fig. 5 *E* and *F*) similarly identified YY1 binding sites located upstream to the D-box and RORE enhancer sites, downstream from the CpG islands, and within the proximal promoter regions. Chip assays revealed the circadian bindings of the YY1 protein to two single cognate sites, respectively located downstream from the CpG island and upstream to the enhancer region, and to a unique site located within the proximal promoter region (*SI Appendix*, Fig. S5 *A–D*). Note that, in both liver and ileum, the same unique YY1 binding site was functional (*i.e.,* bound the YY1 protein) within the proximal promoter regions of D-box and RORE genes (*SI Appendix*, Fig. S6 *C* and *D*).

Taken altogether, our above data show i) that the YY1 protein binds, in a circadian manner, to its two YY1 cognate sites located, respectively, upstream to the enhancer and downstream from the CpG island and ii) that the same enhancer–mediator components (e.g., CBP, P300, RNAPII, BRD4, and MED proteins) are associated within a region that includes both the enhancer–mediator complex and its cognate CpG island. Knowing that a "YY1 protein dimerization" is involved in the generation of loops between enhancer and promoter regions (48), our data indicate that before the start of gene transcription, a circadian dimerization occurs between YY1 proteins bound upstream to the enhancers and downstream from the CpG islands. Furthermore, among the several YY1 consensus sites present within the proximal promoter region, a single one (Fig. 5 *A* and *B*) was found to bind the YY1 protein, indicating that the unbound sites (Fig. 5 *A* and *B*) could be involved in additional "Circadian Clock-controlled" events. We suggest that the "unbound YY1 sites" located near the TSS could be functional at time points which are not included in our study and may interact with either i) the 3′ YY1 site located downstream from the intronic CpG islands, thereby allowing a direct transfer of CpG island components to the TSS region and/or ii) to the 5′ YY1 site located upstream to the enhancer–mediator region, thereby allowing a transfer of components to the TSS region, or iii) could possibly be involved in YY1-guided interactions with genes located on either the same or different chromosomes.

Functionally Similar CpG Islands Are Present within BMAL1-Dependent Circadian Clock-Controlled (CC) Output Genes. All BMAL1-activated genes contain two cognate YY1 binding sites located upstream to their E-box enhancer and downstream to their CpG island, together with several YY1 sites within their proximal promoter regions (Fig. 5*G*). Chip analyses revealed a circadian YY1 recruitment to single cognate sites located upstream to the E-box enhancer and downstream from the CpG island, as well as to a unique binding site within the proximal promoter region (*SI Appendix*, Fig. S6*H*), all of which lacking in BMAL1$^{hep-/-}$mice (*SI Appendix*, Fig. S6*F*). Note also that the bindings of the YY1 protein to cognate sites located near the CpG islands and E-box enhancers preceded its binding to the "active" YY1 site located within the proximal promoter region (*SI Appendix*, Fig. S6*G*).

Chip analyses revealed at ZT8, but not at ZT20, the circadian presence of BMAL1 on CpG islands (Fig. 3*C*), even though these islands lack an E-box sequence. Further analyses indicated that components of activating complex (H3K27Ac, H3K4Me1, RNAPII, CBP, P300, and MED12; see Figs. 2*E* and 3 *F* and *K*), similar to those present on CpG islands of RORE and D-box genes, were also present on CpG islands of BMAL1-dependent E-box genes.

Unlike the YY1 Protein, the Protein CTCF Is not Involved in Interactions between the Enhancer, the Promoter, and the CpG Island of CC Output Genes. In eukaryotes, the boundaries of most genomic topologically associated domains (TAD's) are characterized by the presence of clusters of convergent CTCF binding sites which are evolutionary conserved and known to be required for TAD's function (49, 50). The CTCF protein is known to be involved in the generation of enhancer–promoter and promoter–promoter loops which are present within the 3D genomic chromatin architecture (51). For some of these genes, CTCF has been shown to cooperate with the cohesin protein complex and to mediate enhancer–promoter and promoter–promoter contacts (52, 53), and for other genes, CTCF acts as a "transcriptional insulator," thereby preventing long-range enhancer-promoter contacts (54).

Interestingly, bioinformatic searches on both D-box (E2F8) and RORE (NDEL1) circadian genes expressed in the mouse liver identified multiple CTCF binding sites located i) upstream to their D-box and RORE enhancers, ii) within the genes and iii) downstream from their transcriptional termination sites (TTS) (*SI Appendix*, Fig. S5*E*). In the human E2F8 and NDEL1 circadian genes, multiple CTCF binding sites were similarly present upstream to their enhancer and downstream from their TTS. However, over a 24 h circadian period (*SI Appendix*, Fig. S5*E*), chip assays carried out with mouse liver extracts did not reveal any significant CTCF bindings to these sites, indicating that these "unoccupied" CTCF sites are not involved in the formation of loops within the CC output genes.

We conclude that it is the YY1 protein, and not the CTCF protein, which is instrumental in the "loop formation" during the period of "gene activation", thereby mediating the interactions of the enhancer with both the CpG island and the promoter region within CC output genes.

The Circadian Bindings of the YY1 Protein to Single Cognate Sites Located Upstream to the Enhancer Region of the "Core Clock" and of Its "Immediate CC Output" Genes, Precede Its Binding to a Unique Active Site Located within Their Proximal Promoter Region. A bioinformatic search within the "core clock" and its immediate CC output genes (all of which lacking an intronic CpG island; see Fig. 4*C* and *SI Appendix*, Table S7) revealed the presence of single YY1 binding sites located in the vicinity of the enhancers of RORE (for BMAL1, RevErbα, and E4BP4 genes; Fig. 5*H*) and D-box (for PER1 and PER2 genes; Fig. 5*I*), as well as several

YY1 binding sites located within their proximal promoter regions (Fig. 6 *H* and *I*; see also Fig. 4*C*). Further chip assays showed that the circadian YY1 recruitments on the "upstream enhancer" preceded the recruitment to a unique YY1 active site located among several inactive sites within the proximal promoter region (Fig. 6*I*). As expected, in BMAL1$^{hep-/-}$ mice in which DBP and RevErbα are not expressed (Fig. 4*C*), the YY1 bindings to cognate sites located upstream to the D-box enhancers and within the proximal promoter regions of PER1 and PER2 were lost (Fig. 6*J*), while YY1 bindings to the cognate sites located near the RORE enhancers and within the proximal promoter regions of BMAL1 and E4BP4 genes were constitutive (Fig. 6*J*).

A Circadian-Active Condensate Is Involved in the Transcriptional Activation of the CC Output Genes. We have shown above (Fig. 1 *A*–*C*) that all CC-controlled output genes contain a single intronic CpG-rich island which exhibits a circadian alternate CpG methylation/demethylation. The CpG demethylation is associated with the enhancer-controlled active phase of gene transactivation, whereas the CpG methylation is concomitant with the rest phase of gene repression, as indicated by the alternate circadian bindings of either the RORγ/DBP transactivators or the RevErbα/E4BP4 transrepressors to their cognate sites (*SI Appendix*, Fig. S1 *C* and *D*; see Fig. 4*C*).

At the end of rest phase-beginning of the activation phase, the removal of a transrepressor (either RevErbα or E4BP4) and the concomitant binding of a cognate transactivator (either RORγ or DBP; see Fig. 3 *A* and *B* and *SI Appendix*, Fig. S4 *A* and *B*) lead, within the islands, to the replacement of the "repressive" methylated histones H3K9Me3 and H3K27Me3 by their "active" acetylated H3K9Ac and H3K27Ac counterparts (Fig. 2 *C*–*E* and *SI Appendix*, Fig. S4 *A* and *B*), thereby resulting in HP1α eviction and the conversion of a "closed" heterochromatin into an "active" euchromatin. This HP1α eviction then leads to the concomitant removal of the DNA methylating enzymes (DNMT3A, MBD4, and MeCP2) and to the demethylation of the CpG islands through the recruitment of the DNA demethylating enzymes (TDGα, APOBEC2, GADD45α, and AID; see Fig. 1 *D* and *E*, and schemes in Fig. 4 *A* and *B* and *SI Appendix*, Fig. S4*A*). Importantly, it also leads to the binding of the YY1 "bridging" protein (Fig. 6 *A* and *B*; see the YY1 section) to two cognate sites, respectively, located upstream to the enhancer and downstream from the demethylated CpG islands, all of which resulting upon YY1 dimerization in a "loop space" that encompasses all DNA sequences present between these two sites (see the schemes in Fig. 4 *A* and *B*). Furthermore, chip analyses reveal, within these islands, the presence of components of enhancer-mediator complexes (i.e., RNAPII, P300, CBP, BRD4, MED1, and MED12; see Fig. 3 *D*, *E*, *G*, and *K* and *SI Appendix*, Figs. S2 *A*, *I*, and *J* and S4*B*), all of which being known to be associated within the enhancer condensate which precedes the initiation of transcription (41, 43–47, 55). Note that the enhancer-specific histones H3.3, H2A.Z, and H3K4Me1 (21) are also present within these demethylated CpG islands (Fig. 2 *C* and *D* and *SI Appendix*, Figs. S2 *M* and *N* and S4*B*).

Thus, it appears that before the pre-mRNA initiation of transcription, a single transcriptionally active demethylated condensate is generated upon dimerization of YY1 proteins bound upstream to the transcriptional enhancer and downstream from the transcriptionally inactive hydrophobic methylCpG-rich island. This "active condensate" comprises demethylated CpGs, the acetylated histone H3K9Ac, and the DNA demethylating enzymes TDGα, APOBEC2, GADD45α, and AID (*SI Appendix*, Fig. S4*A*). It is also enriched in both transactivators (either RORγ or DBP), histone demethylases (JARID1A, KDM6A, and JHDM3), and enhancer-specific histones (H3K27Ac, H3K4Me1, H3.3, and H2A.Z), which, together with several components of enhancer–mediator complexes (e.g., RNAPII, P300, CBP, BRD4, MED1, and MED12), are assembled on enhancers (either a RORE or a D-box), before being transferred to demethylated CpG islands upon YY1 protein dimerization (*SI Appendix*, Fig. S4*B*). Upon the binding of a transactivator (RORγ or DBP) to its cognate enhancer (a RORE or a D-Box) followed by the subsequent dimerization of the two YY1 proteins which are, respectively, bound upstream to the enhancer and downstream from the CpG island (Figs. 5 *A* and *B* and 6 *A* and *B*), the same active biomolecular condensate components are concomitantly associated for 8 h within the loop that includes the transcriptional enhancer and the demethylated CpG island (see above). In other words, our data are in keeping with the presence (for a minimum period of 8 h) of a single transcriptionally active condensate that encompasses both the enhancer–mediator region and the CpG island (Fig. 5*J*).

Taking our above data altogether, we propose that during the active phase of the circadian cycle, a distinct circadian active condensate is involved in the transcriptional control of activation of the CC-controlled genes, through modulation of the local concentrations in activating components which, within the enhancer region, are sequentially involved as transactivators (RORγ or DBP; see *SI Appendix*, Fig. S4*B*). Before the initiation of transcription of the pre-mRNAs, the CpG islands are demethylated (Fig. 4 *A* and *B*) and, upon dimerization of the 5′-enhancer and 3′-island YY1 sites, start to store components of the enhancer/mediator preinitiation complexes assembled under the circadian control of either the RORγ or the DBP transactivator, thereby generating a single circadian transcriptionally active condensate (see above and *SI Appendix*, Fig. S4*B*). This generation creates a propitious environment for further storing enhancer/mediator-originated components during the next 4 h (i.e., transactivators, histone demethylases, H3K27Ac, H3K4Me1, H3.3 and H2A.Z histones, RNAPII, P300, CBP, BRD4, MED1, and MED12; *SI Appendix*, Fig. S4*B*). Importantly, all of these condensate components are still present during the next 4 h (see *SI Appendix*, Fig. S4 and figures referenced therein), whereas all of them have disappeared during the last 4 h of the pre-mRNA transcription period (*SI Appendix*, Fig. S4). Of note, this disappearance of the island condensate during the last 4 h of pre-mRNA transcription may reflect (i) the use of enhancer-mediator components which are stored in the island for the synthesis of the pre-mRNA during the last 4 h of its transcription, (ii) a circadian progressive disappearance of RORγ and DBP transactivators upon the circadian bindings of the RevErbα and E4BP4 transrepressors or (iii) a local accumulation of a high concentration of negatively charged RNA during the pre-mRNA stage of transcription and elongation, as suggested by Henninger et al. (56).

To conclude, our data indicate that during the circadian phase of gene activation, the demethylation of the intronic CpG islands is involved in boosting the transcriptional activation of the CC output genes, upon the alternate circadian binding of transactivators and transrepressors to their cognate binding sites.

How Could the Circadian Demethylation of the CpG-Rich Islands Be Impaired upon Aging? We have shown above, in the section entitled "*The alternate demethylation–methylation of the intronic CpG-rich islands is controlled by the circadian core clock,*" that upon the concomitant circadian binding of the DNA demethylating enzymes (TDGα, GADD45α, AID, and Apobec2; see Fig. 1 *D* and *E*), the CpG islands are fully demethylated in 8-wk-old adult mice during the 12-h period of activation of D-box and RORE genes (see *SI Appendix*, Fig. S3 *A* and *B* for the circadian demethylation/methylation; see also Fig. 4 *A* and *B*). In contrast, during the 12-h period of gene repression, the same islands are fully methylated (see

SI Appendix, Fig. S3 *A* and *B*) upon binding of the DNA methylating enzymes DNMT3a, MBD4, and MeCP2 (Fig. 1 *D* and *E*).

Interestingly, it has been proposed that, upon aging, the genomic methylCpG demethylation is impaired during the active phase, thus leading to an increased level of CpG methylation and to a reduced expression of circadian genes (for reviews, see refs. 57 and 58 and references therein). We have now demonstrated that the CpG island demethylation is dependent on three crucial circadian steps (Fig. 4 *A* and *B*), i.e., i) the removal of a transrepressor (RevErbα or E4BP4; Fig. 1 *H* and *I*, and *SI Appendix*, Fig. S1 *C* and *D*), ii) the binding of a transactivator (either RORγ or DBP; Fig. 1*H* and *SI Appendix*, Fig. S1 *C* and *D*) to its cognate-site, and iii) the removal of the HP1α protein (Figs. 4 *A* and *B* and 2 *A* and *B* of our accompanying paper (59) entitled "*The HP1α protein is mandatory to repress the circadian clock and its output genes during the 12h period of transcriptional repression*"), all of which resulting in an increased activity of the DNA demethylating enzymes (Fig. 1 *D* and *E*). Thus, an impairment in any of the above three steps during the circadian period of gene activation could lead to an increased methylation of the CpG-rich islands (Fig. 4 *A* and *B*), similar to that known to occur upon aging (57, 58). Of note, this impairment in the demethylation of the CpG islands during the "active phase" could subsequently lead to an impaired storage capacity of the CpG islands and to a decreased initiation of transcription of the CC output genes, similar to those observed upon aging and various age-related pathological conditions (57, 58). In this respect, we note that Clarkson-Townsend et al. (23) recently reported that a "*Maternal circadian disruption is associated with variation in placental DNA methylation.*"

Taking our data altogether, we conclude that during youth, the circadian demethylation of the CpG islands is fully functional, while impaired upon aging during the transcriptional "activation phase" which controls the demethylation of the CpG islands (Fig. 4 *A* and *B*). This aging impairment in the circadian demethylation could then lead to an increased methylation of the CpG islands upon premature aging, due to an impaired activity of the DNA demethylating enzymes (TDGα, GADD45α, AID, and Apobec2). We propose that such an impairment could be cured/prevented upon boosting the transcriptional activation phase through increasing the activity of the DNA demethylating enzymes, which suggests that the "eye vision restoration" recently reported by Lu et al. (60) could involve a similar "deoxymethyl-CpG demethylation" mechanism.

Materials and Methods

Mice Models.

Mice. First, 8 to 12-wk-old C57BL6/J male wild-type (WT) mice were from Charles River Laboratories. The mice were provided food and water ad libitum, under 12-h light (6 AM to 6 PM; ZT0–ZT12) and 12-h dark (6 PM to 6 AM; ZT12–ZT0) conditions. Hepatocyte-specific ablation of Bmal1 (Bmal1$^{hep-/-}$), RevErbα (RevErbα $^{hep-/-}$), RORα/RORγ (RORα/RORγ $^{hep-/-}$), and E4BP4 (E4BP4 $^{hep-/-}$) was generated by crossing "floxed" female mice with albumin-CreERT^2 "floxed" male mice (61), and subsequent tamoxifen injections were given for 5 d. Bmal1-floxed mice were obtained from Jackson Laboratories (B6.129S4 (Cg)-Arntl^{tm1Weit}/J), whereas all other floxed mice were generated and maintained in Institut de Génétique et de Biologie Moléculaire et Cellulaire (IGBMC)/Institut Clinique de la Souris (ICS). Genotyping was performed by PCR on genomic DNA isolated from mouse tails. All experiments were performed under light–dark (L/D) conditions, with ZT0 being the start of the light period (6 AM) and ZT12 the start of the dark period (6 PM). Mice were killed at a 4-h interval starting at ZT0. All mice were fed a normal laboratory chow diet. Breeding, maintenance, and experimental manipulations were approved by the Animal care and Use Committee of IGBMC/ICS.

Mutant Mice Strains. Mouse: C57BL/6J (Charles River laboratories), Mouse: Alb-CreERT^2/E4BP4 $^{hep-/-}$ [Mouse Clinical Institute (ICS)], Mouse: Alb-CreERT^2/BMAL1 $^{hep-/-}$ [Jackson laboratories B6.129S4 (Cg)-Arntltm1Weit/J], Mouse: Alb-CreERT^2/RevErbα $^{hep-/-}$ [Mouse Clinical Institute (ICS)], and Mouse: Alb-CreERT^2/RORα/RORγ $^{hep-/-}$ [Mouse Clinical Institute (ICS)].

Data, Materials, and Software Availability. MeDIP-seq deposited data from liver and Ileum samples of WT mouse are available under GEO Accession no: GSE182147. All study data are included in the article and/or *SI Appendix*.

ACKNOWLEDGMENTS. We thank Professor Paul Mandel (1908-1992), and those who worked and published with Professor Pierre Chambon over the last 60 years. We are grateful to Valérie Schon for excellent secretarial help and thank the staff of the animal house facilities in the Institut de Génétique et de Biologie Moléculaire et Cellulaire (IGBMC) and the Institut de la Clinique de la Souris (ICS). This work was supported by the Centre National de la Recherche Scientifique (CNRS), the Institut National de la Santé et de la Recherche Médicale (INSERM), the University of Strasbourg Institute for Advanced Studies (USIAS), and the Association pour la Recherche à l'IGBMC (ARI). N.M. and M.D. were supported by ARI fellowships.

Author affiliations: [a]Institut de Génétique et de Biologie Moléculaire et Cellulaire, CNRS Unité Mixte de Recherche 7104, INSERM U1258, 67404 Illkirch, France; [b]University of Strasbourg Institute for Advanced Study, 67404 Illkirch, France; and [c]Collège de France, Illkirch 67404, France

1. R. Holliday, J. E. Pugh, DNA modification mechanisms and gene activity during development. *Science* **187**, 226–232 (1975).
2. A. D. Riggs, X inactivation, differentiation, and DNA methylation. *Cytogenet. Cell Genet.* **14**, 9–25 (1975), 10.1159/000130315.
3. A. Zemach, I. E. McDaniel, P. Silva, D. Zilberman, Genome-wide evolutionary analysis of eukaryotic DNA methylation. *Science* **328**, 916–919 (2010), 10.1126/science.1186366.
4. E. Li, T. H. Bestor, R. Jaenisch, Targeted mutation of the DNA methyltransferase gene results in embryonic lethality. *Cell* **69**, 915–926 (1992), 10.1016/0092-8674(92)90611-f.
5. M. Okano, D. W. Bell, D. A. Haber, E. Li, DNA methyltransferases Dnmt3a and Dnmt3b are essential for de novo methylation and mammalian development. *Cell* **99**, 247–257 (1999), 10.1016/s0092-8674(00)81656-6.
6. A. C. Ferguson-Smith, H. Sasaki, B. M. Cattanach, M. A. Surani, Parental-origin-specific epigenetic modification of the mouse H19 gene. *Nature* **362**, 751–755 (1993), 10.1038/362751a0.
7. A. Bird, M. Taggart, M. Frommer, O. J. Miller, D. Macleod, A fraction of the mouse genome that is derived from islands of nonmethylated, CpG-rich DNA. *Cell* **40**, 91–99 (1985), 10.1016/0092-8674(85)90312-5.
8. C. P. Walsh, J. R. Chaillet, T. H. Bestor, Transcription of IAP endogenous retroviruses is constrained by cytosine methylation. *Nat. Genet.* **20**, 116–117 (1998), 10.1038/2413.
9. J. Borgel *et al.*, Targets and dynamics of promoter DNA methylation during early mouse development. *Nat. Genet.* **42**, 1093–1100 (2010), 10.1038/ng.708.
10. A. P. Bird, A. P. Wolffe, Methylation-induced repression–belts, braces, and chromatin. *Cell* **99**, 451–454 (1999), 10.1016/s0092-8674(00)81532-9.
11. A. M. Deaton, A. Bird, CpG islands and the regulation of transcription. *Genes. Dev.* **25**, 1010–1022 (2011), 10.1101/gad.2037511.
12. Y. Tao *et al.*, Lsh, chromatin remodeling family member, modulates genome-wide cytosine methylation patterns at nonrepeat sequences. *Proc. Natl. Acad. Sci. U.S.A.* **108**, 5626–5631 (2011), 10.1073/pnas.1017000108.
13. F. Fuks, W. A. Burgers, A. Brehm, L. Hughes-Davies, T. Kouzarides, DNA methyltransferase Dnmt1 associates with histone deacetylase activity. *Nat. Genet.* **24**, 88–91 (2000), 10.1038/71750.
14. M. Weber *et al.*, Distribution, silencing potential and evolutionary impact of promoter DNA methylation in the human genome. *Nat. Genet.* **39**, 457–466 (2007), 10.1038/ng1990.
15. Y. Yin *et al.*, Impact of cytosine methylation on DNA binding specificities of human transcription factors. *Science* **356**, 2239 (2017), 10.1126/science.aaj2239.
16. S. Panda, Circadian physiology of metabolism. *Science* **354**, 1008–1015 (2016), 10.1126/science.aah4967.
17. J. Bass, M. A. Lazar, Circadian time signatures of fitness and disease. *Science* **354**, 994–999 (2016), 10.1126/science.aah4965.
18. J. S. Takahashi, Transcriptional architecture of the mammalian circadian clock. *Nat. Rev. Genet.* **18**, 164–179 (2017), 10.1038/nrg.2016.150.
19. H. A. Duong, M. S. Robles, D. Knutti, C. J. Weitz, A molecular mechanism for circadian clock negative feedback. *Science* **332**, 1436–1439 (2011), 10.1126/science.1196766.
20. S. Katada, P. Sassone-Corsi, The histone methyltransferase MLL1 permits the oscillation of circadian gene expression. *Nat. Struct. Mol. Biol.* **17**, 1414–1421 (2010), 10.1038/nsmb.1961.
21. N. Koike *et al.*, Transcriptional architecture and chromatin landscape of the core circadian clock in mammals. *Science* **338**, 349–354 (2012), 10.1126/science.1226339.
22. A. Azzi *et al.*, Circadian behavior is light-reprogrammed by plastic DNA methylation. *Nat. Neurosci.* **17**, 377–382 (2014), 10.1038/nn.3651.
23. D. A. Clarkson-Townsend *et al.*, Maternal circadian disruption is associated with variation in placental DNA methylation. *PLoS One* **14**, e0215745 (2019), 10.1371/journal.pone.0215745.
24. J. R. Beytebiere *et al.*, Tissue-specific BMAL1 cistromes reveal that rhythmic transcription is associated with rhythmic enhancer-enhancer interactions. *Genes. Dev.* **33**, 294–309 (2019), 10.1101/gad.322198.118.
25. X. Yang *et al.*, Nuclear receptor expression links the circadian clock to metabolism. *Cell* **126**, 801–810 (2006), 10.1016/j.cell.2006.06.050.

26. A. Mukherji, A. Kobiita, T. Ye, P. Chambon, Homeostasis in intestinal epithelium is orchestrated by the circadian clock and microbiota cues transduced by TLRs. *Cell* **153**, 812–827 (2013), 10.1016/j.cell.2013.04.020.
27. B. Fang *et al.*, Circadian enhancers coordinate multiple phases of rhythmic gene transcription in vivo. *Cell* **159**, 1140–1152 (2014), 10.1016/j.cell.2014.10.022.
28. J. D. Lewis *et al.*, Purification, sequence, and cellular localization of a novel chromosomal protein that binds to methylated DNA. *Cell* **69**, 905–914 (1992), 10.1016/0092-8674(92)90610-o.
29. S. Cortellino *et al.*, Thymine DNA glycosylase is essential for active DNA demethylation by linked deamination-base excision repair. *Cell* **146**, 67–79 (2011), 10.1016/j.cell.2011.06.020.
30. K. Arab *et al.*, GADD45A binds R-loops and recruits TET1 to CpG island promoters. *Nat. Genet.* **51**, 217–223 (2019), 10.1038/s41588-018-0306-6.
31. L. DiTacchio *et al.*, Histone lysine demethylase JARID1a activates CLOCK-BMAL1 and influences the circadian clock. *Science* **333**, 1881–1885 (2011), 10.1126/science.1206022.
32. Y. Atlasi, H. G. Stunnenberg, The interplay of epigenetic marks during stem cell differentiation and development. *Nat. Rev. Genet.* **18**, 643–658 (2017), 10.1038/nrg.2017.57.
33. K. Hyun, J. Jeon, K. Park, J. Kim, Writing, erasing and reading histone lysine methylations. *Exp. Mol. Med.* **49**, e324 (2017), 10.1038/emm.2017.11.
34. P. Chen *et al.*, H3.3 actively marks enhancers and primes gene transcription via opening higher-ordered chromatin. *Genes. Dev.* **27**, 2109–2124 (2013), 10.1101/gad.222174.113.
35. P. B. Talbert, M. P. Meers, S. Henikoff, Old cogs, new tricks: The evolution of gene expression in a chromatin context. *Nat. Rev. Genet.* **20**, 283–297 (2019), 10.1038/s41576-019-0105-7.
36. A. Armache *et al.*, Histone H3.3 phosphorylation amplifies stimulation-induced transcription. *Nature* **583**, 852–857 (2020), 10.1038/s41586-020-2533-0.
37. J. S. Menet, S. Pescatore, M. Rosbash, CLOCK:BMAL1 is a pioneer-like transcription factor. *Genes. Dev.* **28**, 8–13 (2014), 10.1101/gad.228536.113.
38. M. Buschbeck, S. B. Hake, Variants of core histones and their roles in cell fate decisions, development and cancer. *Nat. Rev. Mol. Cell Biol.* **18**, 299–314 (2017), 10.1038/nrm.2016.166.
39. J. Soutourina, Transcription regulation by the mediator complex. *Nat. Rev. Mol. Cell Biol.* **19**, 262–274 (2018), 10.1038/nrm.2017.115.
40. L. El Khattabi *et al.*, A pliable mediator acts as a functional rather than an architectural bridge between promoters and enhancers. *Cell* **178**, 1145–1158.e1120 (2019), 10.1016/j.cell.2019.07.011.
41. W. K. Cho *et al.*, Mediator and RNA polymerase II clusters associate in transcription-dependent condensates. *Science* **361**, 412–415 (2018), 10.1126/science.aar4199.
42. Y. H. Kim *et al.*, Rev-erbalpha dynamically modulates chromatin looping to control circadian gene transcription. *Science* **359**, 1274–1277 (2018), 10.1126/science.aao6891.
43. A. Boija *et al.*, Transcription factors activate genes through the phase-separation capacity of their activation domains. *Cell* **175**, 1842–1855.e1816 (2018), 10.1016/j.cell.2018.10.042.
44. A. V. Zamudio *et al.*, Mediator condensates localize signaling factors to key cell identity genes. *Mol. Cell* **76**, 753–766.e756 (2019), 10.1016/j.molcel.2019.08.016.
45. Y. E. Guo *et al.*, Pol II phosphorylation regulates a switch between transcriptional and splicing condensates. *Nature* **572**, 543–548 (2019), 10.1038/s41586-019-1464-0.
46. K. Shrinivas *et al.*, Enhancer features that drive formation of transcriptional condensates. *Mol. Cell* **75**, 549–561.e547 (2019), 10.1016/j.molcel.2019.07.009.
47. B. R. Sabari *et al.*, Coactivator condensation at super-enhancers links phase separation and gene control. *Science* **361**, 3958 (2018), 10.1126/science.aar3958.
48. A. S. Weintraub *et al.*, YY1 is a structural regulator of enhancer-promoter loops. *Cell* **171**, 1573–1588.e1528 (2017), 10.1016/j.cell.2017.11.008.
49. S. S. P. Rao *et al.*, A 3D map of the human genome at kilobase resolution reveals principles of chromatin looping. *Cell* **159**, 1665–1680 (2014), 10.1016/j.cell.2014.11.021.
50. E. Kentepozidou *et al.*, Clustered CTCF binding is an evolutionary mechanism to maintain topologically associating domains. *Genome. Biol.* **21**, 5 (2020), 10.1186/s13059-019-1894-x.
51. R. G. Arzate-Mejía, F. Recillas-Targa, V.G. Corces, Developing in 3D: The role of CTCF in cell differentiation. *Development* **145**, dev137729 (2018), 10.1242/dev.137729.
52. N. Kubo *et al.*, Promoter-proximal CTCF binding promotes distal enhancer-dependent gene activation. *Nat. Struct. Mol. Biol.* **28**, 152–161 (2021).
53. Q. Szabo *et al.*, Regulation of single-cell genome organization into TADs and chromatin nanodomains. *Nat. Genet.* **52**, 1151–1157 (2020).
54. H. Huang *et al.*, CTCF mediates dosage- and sequence-context-dependent transcriptional insulation by forming local chromatin domains. *Nat. Genet.* **53**, 1064–1074 (2021).
55. B. R. Sabari, A. Dall'Agnese, R. A. Young, Biomolecular condensates in the nucleus. *Trends Biochem. Sci.* **45**, 961–977 (2020), 10.1016/j.tibs.2020.06.007.
56. J. E. Henninger *et al.*, RNA-mediated feedback control of transcriptional condensates. *Cell* **184**, 207–225.e224 (2021).
57. S. Horvath, R. Kenneth, DNA methylation-based biomarkers and the epigenetic clock theory of ageing. *Nat. Rev. Genet.* **19**, 371–384 (2018), 10.1038/s41576-018-0004-3.
58. A. E. Field *et al.*, DNA methylation clocks in aging: Categories, causes, and consequences. *Mol. Cell* **71**, 882–895 (2018).
59. N. Misra, M. Damara, P. Chambon, The HP1αprotein is mandatory to repress the circadian clock and its output genes during the 12h period of transcriptional repression, in press.
60. Y. Lu *et al.*, Reprogramming to recover youthful epigenetic information and restore vision. *Nature* **588**, 124–129 (2020).
61. M. Schuler, A. Dierich, P. Chambon, D. Metzger, Efficient temporally controlled targeted somatic mutagenesis in hepatocytes of the mouse. *Genesis* **39**, 167–172 (2004).